2011 American Control Conference
on O'Farrell Street, San Francisco, CA, USA
June 29 - July 01, 2011

Predictive and Sliding Mode Cascade Control for Unmanned Surface Vessels

Lucas C. McNinch and Hashem Ashrafiuon
Center for Nonlinear Dynamics and Control
Villanova University, Villanova, PA 19085 USA

Abstract— **This paper presents an optimizing sliding mode cascade control structure that determines the optimal sliding surface parameters for sliding mode control of underactuated Unmanned Surface Vessel systems. A discrete-time, nonlinear model predictive controller is used to update the parameters of the sliding mode control surfaces in order to achieve a specified performance objective such as minimum tracking error, minimum time or minimum energy. The determination of these surface parameters is subject to constraints that arise from the stability conditions imposed by the sliding mode control law and the physical limits on the system such as input saturation. Examples are presented to verify the superior performance of the cascade control structure compared with the original sliding mode control.**

I. Introduction

Sliding mode control [1] has been shown to be a robust and effective control approach for underactuated nonlinear systems. In an effort to avoid excessive control action and/or achieve faster reaching times to the sliding surface, previous research has focused on methods to optimally redefine the sliding surfaces. Salamci, et al. [2] approximate the nonlinear system by a LTV (linear time varying) system and design LTV optimal sliding surfaces to minimize the desired objective function based on a weighted combination of the system states and controls. Eksin, et al. [3] present an approach for designing time-varying nonlinear sliding surfaces for second-order systems in order to minimize the settling time. In this method, the proposed sliding surface is the combination of the classical linear sliding surface and an adaptive time-varying nonlinear part. Kim and Park [4] present a method for designing a sliding mode control law to minimize quadratic cost functions. The method is based on manipulation of the linear matrix inequalities (LMIs) imposed by the design objective.

The optimal design of sliding surfaces for underactuated nonlinear systems has received less attention. Nikkhah, et al. [5] proposed an optimization based approach for set-point control of underactuated systems with isolated equilibrium points which was later used for a cascade control structure to improve performance [6]. This method is expanded to trajectory tracking control for Unmanned Surface Vessel (USV) systems in [7]. Optimal design can be a critical aspect for the implementation of sliding mode control to underactuated systems because the influence of the controls in these nonlinear systems is, in general, limited. Because of this limitation, it may require long reaching times and/or undesirable state trajectories to reach the final state target [8].

In this paper, an optimal sliding surface design methodology for a nonlinear underactuated USV system is developed by incorporating principles from nonlinear predictive control that have been widely applied to nonlinear systems [9]. Although we consider an underactuated USV system in this work, the proposed approach is also applicable to fully actuated systems without modification. We determine the time-invariant parameters of the sliding mode controller developed in [10] by minimizing a specified performance objective under sliding mode control. Constraints in this minimization include satisfying limits on the control, restrictions on the parameters, and any dynamic restrictions on the state trajectory. The result is a nonlinear optimization problem similar to that posed in nonlinear predictive control except that the decision variables are the sliding mode control parameters as opposed to the actual control trajectory.

There are a number of advantages to the proposed approach. Common performance objectives, such as minimum energy and minimum time, can easily be incorporated into the sliding mode control framework for underactuated systems. Physical constraints such as actuator saturation limits are easily implemented. Undesirable state trajectories can be eliminated through the use of dynamic state constraints in the optimization problem. If the resulting nonlinear optimization problem is feasible, the sliding mode controller will avoid these trajectories. If the optimization problem is infeasible, then the system is over specified and it is not possible to avoid the specified state trajectories. In this case, either the constraints on the control actuation, the constraints on the dynamic state trajectory, or both must be relaxed in order to obtain a feasible optimization problem.

II. USV System Model

The 3-DOF planar model of a surface vessel shown in Figure 1 is considered in this work. This model includes surge, sway, and yaw motion with two propeller force inputs f_1 and f_2. The geometrical relationship between the inertial reference frame and the vessel-based body-fixed frame (located at the vessel center of mass) is defined in terms of velocities as

$$\dot{x} = v_x \cos\theta - v_y \sin\theta \tag{1}$$

$$\dot{y} = v_x \sin\theta + v_y \cos\theta \tag{2}$$

$$\dot{\theta} = \omega \tag{3}$$

where x and y denote the position of the center of mass, θ is the orientation angle of the vessel in the inertial

978-1-4577-0079-8/11/$26.00 ©2011 AACC

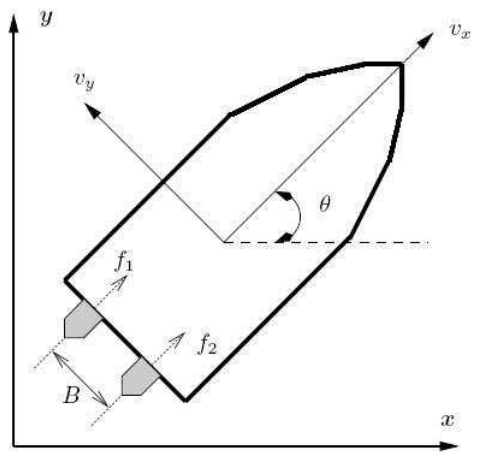

Fig. 1. Planar surface vessel schematic.

reference frame, v_x and v_y are the surge and sway velocities, respectively, and ω is the angular velocity of the vessel.

In the body-fixed frame, the nonlinear equations of motion for a simplified model of the dynamics of a surface vessel, where motion in heave, roll, and pitch are neglected, are given by

$$m_{11}\dot{v}_x - m_{22}v_y\omega + d_1 v_x^{\alpha 1} = f \tag{4}$$

$$m_{22}\dot{v}_y + m_{11}v_x\omega + d_2\,\mathrm{sgn}(v_y)|v_y|^{\alpha_2} = 0 \tag{5}$$

$$m_{33}\dot{\omega} + m_d v_x v_y + d_3\,\mathrm{sgn}(\omega)|\omega|^{\alpha_3} = T \tag{6}$$

where m_{ii} are the mass and inertial parameters and $m_d = m_{22} - m_{11} > 0$. The m_{ii} parameters include added mass contributions that represent hydraulic pressure forces and torque due to forced harmonic motion of the vessel which are proportional to acceleration. The hydrodynamic damping is modeled using a power law expression in Equations (4)–(6). This dynamic model is widely used in the literature and a more detailed discussion can be found in [11]. In this work, only forward vessel motion, $v_x > 0$, is considered because the forward and reverse motion dynamics are quite different. The surge control force f and the yaw control moment T are given in terms of the two propeller forces as

$$\begin{aligned} f &= f_1 + f_2 \\ T &= B(f_2 - f_1)/2 \end{aligned} \tag{7}$$

where B is the lateral distance between the propellers. The USV model parameters in Equations (4)–(6) are presented in Table II. These mass and damping terms were determined through experimental system identification tests carried out on this vessel [12] and are assumed to remain constant.

III. Sliding Mode Control Formulation

The trajectory tracking sliding mode control law for autonomous surface vessels is developed using two sliding surfaces for calculation of the two propeller forces [10]. The first sliding surface is a first-order surface defined in terms of the surge motion tracking errors. The second sliding surface is a second-order surface defined in terms of the lateral motion tracking errors.

TABLE I
Estimated USV system model parameters

Parameter	*Value*
m_{11}	1.96 ± 0.019 kg
d_1	2.44 ± 0.023
α_1	1.51 ± 0.0075
m_{22}	2.40 ± 0.12 kg
d_2	13.0 ± 0.30
α_2	1.75 ± 0.013
m_{33}	0.0430 ± 0.0068 kg
d_3	0.0564 ± 0.00085
α_3	1.59 ± 0.0285

A. Reference Trajectory Determination

The sliding mode controller is designed to track a continuously differentiable trajectory. The trajectory is defined using a set of two ODEs in terms of the two planar global position variables x and y

$$\dot{x}_i = f_i(x_1, x_2, t), \quad f_i : D_i \to \Re^2, \quad i = 1, 2 \tag{8}$$

where x_1 and x_2 are the state variables, D_i is an open and connected subset of $\Re^2$, and f_i is a locally Lipschitz map from D_i into $\Re^2$. The state variables x_1 and x_2 are defined as

$$\begin{aligned} x_1 &= x - x^t \\ x_2 &= y - y^t \end{aligned} \tag{9}$$

where $x^t(t)$ and $y^t(t)$ denote the target trajectory in the inertial reference frame. The functions f_1 and f_2 in Equation (8) are determined based on the desired trajectory dynamics. The exponentially stable target tracking trajectory is defined by the following linear ODE system

$$\begin{aligned} \dot{x}_1 &= -k_1 x_1, \quad k_1(t) > 0 \\ \dot{x}_2 &= -k_2 x_2, \quad k_2(t) > 0 \end{aligned} \tag{10}$$

where the initial conditions are determined based on the initial USV and target positions.

The desired state trajectories in the inertial reference frame are related to the corresponding surge and lateral desired velocities as follows

$$v_x^d = \dot{x}^d \cos\theta + \dot{y}^d \sin\theta \tag{11}$$

$$v_y^d = -\dot{x}^d \sin\theta + \dot{y}^d \cos\theta \tag{12}$$

where $\dot{x}^d = \dot{x}_1 + \dot{x}^t$ and $\dot{y}^d = \dot{x}_2 + \dot{y}^t$.

B. Surge Control Law

The first sliding surface is a first-order exponentially stable surface defined in terms of the vessel's surge motion tracking errors

$$s_1 = \tilde{v}_x + \lambda_1 \int_0^t \tilde{v}_x(\tau)d\tau, \quad \lambda_1 > 0 \tag{13}$$

where " ˜ " denotes the difference between the actual and desired values; *i.e.*, $\tilde{v}_x = v_x - v_x^d$. Note that the integral of v_x is used since position variables cannot be defined in the body-fixed frame. Hence, the desired motion is specified in the inertial reference frame and related to the desired surge and sway velocities and accelerations by Equations (11) and (12).

The sliding mode control law is derived by subtracting a high-slope saturation function from the nominal control as in [13]

$$f = \hat{f} - k_1 \text{sat}(s_1/\epsilon_1) \tag{14}$$

$$\text{sat}(s_1/\epsilon_1) = \begin{cases} s_1/\epsilon_1, & |s_1| \leq \epsilon_1 \\ \text{sgn}(s_1), & |s_1| > \epsilon_1 \end{cases} \tag{15}$$

$$\hat{f} = -\hat{m}_{22} v_y \omega + \hat{d}_1 v_x^{\alpha_1} - \hat{m}_{11} \dot{s}_{r1} \tag{16}$$

$$\dot{s}_{r1} = -\dot{v}_x^d + \lambda_1 \tilde{v}_x \tag{17}$$

where " $\hat{}$ " is used to indicate the estimated model parameters and ϵ_1 is a positive constant which defines a small boundary layer around the surface.

The coefficient k_1 is selected by first defining a Lyapunov candidate function that guarantees reaching the set $\{s_1 \in \Re : |s_1| \leq \epsilon_1\}$ in finite time and remain inside this set thereafter.

$$V_1 = \frac{1}{2} m_{11} s_1^2 \tag{18}$$

The time derivative of Equation (18) can be derived as presented in [10] where the following reaching condition is achieved

$$\dot{V}_1 = m_{11} s_1 \dot{s}_1 \leq -\hat{m}_{11} \eta_1 |s_1|, \quad \eta_1 > 0 \tag{19}$$

if k_1 is selected as

$$k_1 = M_{22} |v_y \omega| + D_1 v_x^{\alpha_1} + M_{11} |\dot{s}_{r1}| + \hat{m}_{11} \eta_1 \tag{20}$$

where M_{ii} and D_i are the bounds for the mass elements and the drag coefficients.

C. Lateral Motion Control Law

The second sliding surface is a second-order exponentially stable surface defined in terms of the vessel's lateral motion tracking errors

$$s_2 = \dot{\tilde{v}}_y + 2\lambda_2 \tilde{v}_y + \lambda_2^2 \int_0^2 \tilde{v}_y(\tau) d\tau, \quad \lambda_2 > 0 \tag{21}$$

where $\tilde{v}_y = v_y - v_y^d$ and $\dot{\tilde{v}}_y = \dot{v}_y - \dot{v}_y^d$. The nominal yaw moment control law is derived for zero dynamics by taking the time derivative of the lateral motion surface and setting it equal to zero and then solving for the yaw moment T

$$\hat{T} = \hat{h}/\hat{b} \tag{22}$$

where " $\hat{}$ " indicates the estimated model and

$$b = m_{22} v_x^d - m_{11} v_x \tag{23}$$

$$\begin{aligned} h = {} & b(m_d v_x v_y + d_3 \,\text{sgn}(\omega) |\omega|^{\alpha_3}) \\ & - (m_{11} v_x \omega + d_2 \,\text{sgn}(v_y) |v_y|^{\alpha_2 - 1}) \\ & + m_{33} \omega (f - d_1 v_x^{\alpha_1} + 2\lambda_2 m_{11} v_x + m_{22} v_y) \\ & + 2\lambda_2 m_{33} d_2 \,\text{sgn}(v_y) + |v_y|^{\alpha_2} \\ & + m_{22} m_{33} (v_r + 2\lambda_2 \dot{v}_y^d - \lambda_2^2 \tilde{v}_y) \end{aligned} \tag{24}$$

$$v_r = (v_y^d \omega - 2\dot{v}_x^d)\omega - \sin\theta \ddot{x}^d + \cos\theta \ddot{y}^d.$$

The yaw moment sliding mode control law is defined using a high-slope saturation function in the same manner as the surge control law

$$T = [\hat{h} - k_2 \text{sat}(s_2/\epsilon_2)]/\hat{b} \tag{25}$$

where the nominal values of b and h are computed by Equations (23) and (24) using the estimated model parameters.

In order to determine k_2, another Lyapunov candidate function is defined

$$V_2 = \frac{1}{2} m_{22} m_{33} s_2^2 \tag{26}$$

which guarantees reaching the set $\{s_2 \in \Re : |s_2| \leq \epsilon_2\}$ in finite time. This Lyapunov function yields the following reaching condition

$$\dot{V}_2 = m_{22} m_{33} s_2 \dot{s}_2 \leq -\hat{m}_{22} \hat{m}_{33} \eta_2 |s_2|, \quad \eta_2 > 0 \tag{27}$$

if k_2 is selected as

$$k_2 = \beta(H + \hat{m}_{22} \hat{m}_{33} \eta_2) + (\beta - 1)|\hat{h}| \tag{28}$$

with H as the bound for the uncertainty in h and β the bound based on the geometric mean of b [10].

IV. Cascade Control

The sliding mode tracking controller presented in Section III computes very quickly but the dynamic performance of the controller is a complex function of the effort, surface, and trajectory parameters. It is difficult to manually determine parameters that yield optimal controller performance for a given scenario, initial conditions, and desired objective function without extensive simulation of the closed-loop system. Another difficulty is that the optimal parameters for one initial condition can yield poor or unacceptable performance for a different initial condition. A significant factor limiting the performance of the USV sliding mode control laws is input saturation. Because sliding mode control considers input constraints through saturation which rarely results in optimal control performance in any multi-input multi-output system. This situation is especially the case for the nonholonomic USV system since the control law calculates a surge force and yaw moment but the saturation is applied to individual propeller inputs. The resulting saturation can lead to increased control chatter that can be detrimental to mechanical actuators. In this work, a multi-rate cascade control structure is presented which optimally adjusts the sliding mode controller parameters using an MPC controller. This cascade structure allows for near-optimal performance while providing a control law that can be computed in real-time and respects input saturation constraints.

A. Cascade Control Structure

A block diagram of the cascade control structure is shown in Figure 2. The primary loop is a discrete-time, nonlinear model predictive controller that re-optimizes the control parameters of the sliding mode controller in the secondary loop at each control interval. The MPC controller executes at a rate that allows the on-line optimization to complete. For this application, the control interval Δt does not need to be fixed. The sliding mode controller computes the control input to the USV system at a rate sufficient to stabilize the system. The model predictive controller is based on a finite

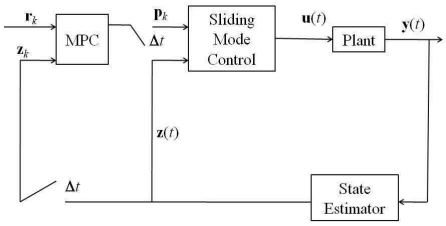

Fig. 2. Controller block diagram

horizon performance objective following the Lagrange cost function in optimal control [14]

$$\min_{\mathbf{p}} J_k = \int_{k\Delta t}^{(k+N)\Delta t} \Phi(\mathbf{z}, \mathbf{u}, t)\, dt \tag{29}$$

where J_k is the objective function value at sample time k, Δt is the control interval, N is the prediction horizon, $\Phi(\cdot)$ is the performance penalty function, $\mathbf{z}$ is the state of the system and $\mathbf{u}$ is the propeller forces determined by the sliding mode controller. This objective is minimized over the surface, effort and trajectory parameters $\mathbf{p}$ subject to the following constraints

$$\dot{\mathbf{z}} = \mathbf{f}(\mathbf{z}, \mathbf{u}, t) \tag{30}$$

$$\mathbf{u} = \begin{bmatrix} f_1 \\ f_2 \end{bmatrix} = \begin{bmatrix} 1 & 1 \\ -B/2 & B/2 \end{bmatrix}^{-1} \begin{bmatrix} f \\ T \end{bmatrix} \tag{31}$$

$$\mathbf{g}(\mathbf{z}, \mathbf{u}) \geq \mathbf{0} \tag{32}$$

$$\mathbf{h}(\mathbf{p}) \geq \mathbf{0} \tag{33}$$

where $\mathbf{f}(\mathbf{z}, \mathbf{u}, t)$ are kinematic and dynamic equality constraints arising from the USV system model Equations (1)–(6), $\mathbf{g}(\mathbf{z}, \mathbf{u})$ is a general inequality constraint on the states and control, and $\mathbf{h}(\mathbf{p})$ is a general inequality constraint on the controller parameters arising from the surface and trajectory derivation. Equation (31) determines the individual propeller forces as a function of surge force f and yaw moment T.

For simplicity, the values of k_1 and k_2 in Equation (10) are defined to be equal; *i.e.*, $k_1 = k_2 = k$. Likewise, the values of the effort parameters η_1 and η_2 in Equations (19) and (27) respectively are defined to be equal; *i.e.*, $\eta_1 = \eta_2 = \eta$. The following input saturation constraints are imposed based on physical constraints of the experimental system.

$$\mathbf{g}_1(\mathbf{u}) = \begin{bmatrix} 0.5 + f_i(t) \\ 1 - f_i(t) \end{bmatrix} \geq \mathbf{0}, \quad i = 1, 2 \tag{34}$$

The four control parameters $\mathbf{p} = [\lambda_1, \lambda_2, \eta, k]^T$ are selected as the decision variables for the optimization subject to the inequality constraints

$$\mathbf{h}(\mathbf{p}) = \mathbf{p} = \begin{bmatrix} \lambda_1 \\ \lambda_2 \\ \eta \\ k \end{bmatrix} \geq \mathbf{0} \tag{35}$$

such that the sliding mode parameters are strictly positive. Minimum tracking error, minimum time and minimum energy performance objectives are considered *and simulation results are presented.*

B. Circular Target Trajectory

The performance of the MPC cascade control structure in this work is compared to that of a base case feasible surface design and an initial optimal surface design. A single optimization of the surface parameters is carried out at time $t = 0$ for the initial optimal surface as in [7]. In the simulation examples, the target follows a circular trajectory centered at $(x = 1\text{m}, y = 2\text{m})$ with a radius of 0.5 meters and constant angular velocity of 0.2 rad/sec (a period of about 30s) beginning at $(x = 1.5\text{m}, y = 2\text{m})$. The USV must approach and track the target from an initial position at $(x = 2\text{m}, y = 1\text{m})$. The desired trajectory $(v_x^d(t), v_y^d(t))$ is generated using the target tracking trajectory presented in Section III-A with trajectory parameter $k = 0.8$. The control parameters are selected as $\lambda_1 = \lambda_2 = 1$, $\epsilon_1 = \epsilon_2 = 0.05$ and $\eta = 0.2$.

1) Minimum Tracking Error Objective: The minimum tracking error objective determines the sliding mode controller parameters that minimize the integral of time multiplied by the squared error (ITSE) cost function

$$\min_{\mathbf{p}} J_k = \int_{k\Delta t}^{(k+N)\Delta t} d^2 t\, dt \tag{36}$$

subject to the kinematic and dynamic equality constraints in Equations (1)–(6), the input saturation constraints in Equation (34) and the parameter constraints in Equation (35) where d is defined as the distance between the center of mass of the USV and the target position.

$$d = \sqrt{(x - x^d)^2 + (y - y^d)^2} \tag{37}$$

The sliding mode control law $\mathbf{u}$ is updated by the model predictive controller at a control interval of $\Delta t = 1$ s and the prediction horizon is $N = 50$.

Figure 3 presents the resulting USV paths for all three cases. Although the path taken is similar to the initial optimization, the increased control input early in the trajectory allows the USV to reach the target more quickly, as demonstrated by the tracking errors shown in Figure 4. The initial optimization yields a 30% performance gain over the base case and the MPC cascade structure yields another 13% cost improvement over the initial optimization. Figure 5 shows the control parameter evolution over the simulation period. Note that the solution to the initial optimization problem is the same as the first control interval in the MPC cascade sequence. Due to the nature of the target tracking trajectory definition, the parameters must be relatively small when the USV is far away from the target such that the control law satisfies the input saturation constraints. However, as is the case with the initial one-time optimization, control input is quickly reduced as the USV moves closer to the target.

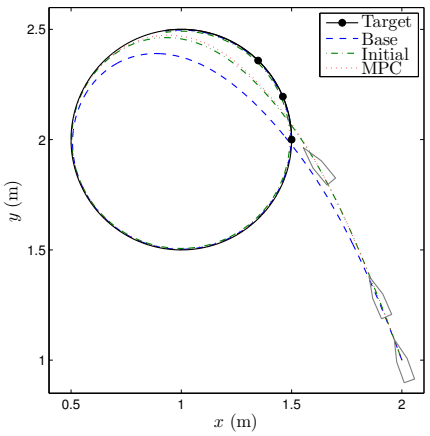

Fig. 3. Simulated minimum error's paths: Circular trajectory

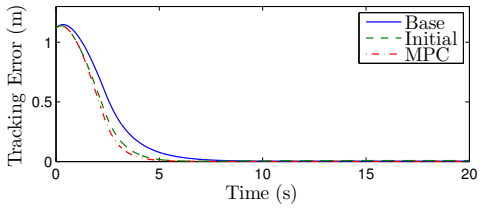

Fig. 4. Minimum error's tracking errors: Circular trajectory

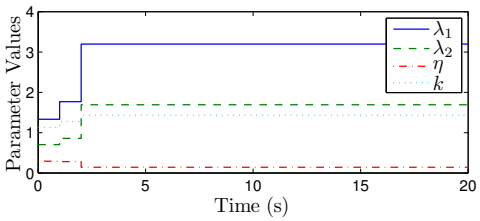

Fig. 5. Minimum error's parameter evolution: Circular trajectory

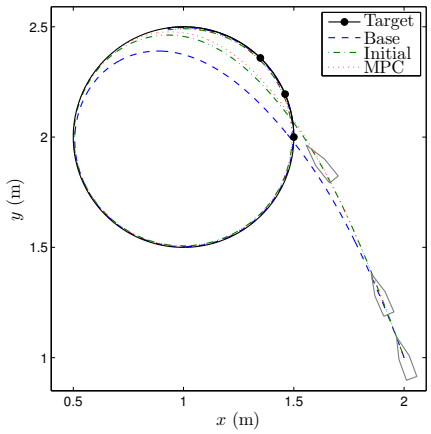

Fig. 6. Simulated minimum time paths: Circular trajectory

2) Minimum Time Objective: The minimum time control objective determines the sliding mode controller parameters that minimize the reach time

$$\min_{\mathbf{p}} J_k = t_{f_k} \tag{38}$$

subject to the kinematic and dynamic equality constraints in Equations (1)–(6), the input saturation constraints in Equation (34) and the parameter constraints in Equation (35) and the following terminal constraint

$$d(\tau) \leq d_{tol}, \quad \tau \geq t_{f_k} \tag{39}$$

where d is the tracking error as defined in Equation (37) and $d_{tol} = 0.01$ m. The sliding mode control law $\mathbf{u}$ is updated by the model predictive controller at a control interval of $\Delta t = 1$ s and the prediction horizon is $N = 50$. Note that the convergence of minimum time problem is not necessarily guaranteed ion its present form, but simulations are presented nonetheless. Figure 6 presents the resulting USV paths for all three cases and figure 7 presents the tracking error d. Figure 8 shows the control parameter evolution over the simulation period. In this case, the initial optimization yields a 31% reduction in reach time over the base case and the MPC cascade structure yields another 12% improvement over the initial optimization.

3) Minimum Energy Objective: The minimum energy objective determines the sliding mode controller parameters that minimize the integral squared control effort cost function

$$\min_{\mathbf{p}} J_k = \int_{k\Delta t}^{(k+N)\Delta t} (f_1^2 + f_2^2)\, dt \tag{40}$$

subject to the reaching time constraint

$$\mathbf{g}_2(\mathbf{z}) = d_{tol} - d(\tau) \geq 0, \quad \tau \geq t_r \tag{41}$$

where t_r is the desired reaching time, and d is the tracking error defined in Equation (37). The reaching time constraint is implemented to force the USV to approach the target trajectory within a specified tolerance, $d_{tol} = 0.01$ m, in a desired reaching time $t_r = 20$ s. Without this reaching time constraint, the minimum energy sliding mode controller approaches the target trajectory too slowly or it may never approach the target at all. As before, the optimization is subject to the kinematic and dynamic equality constraints in Equations (1)–(6), the input saturation constraints in Equation (34) and the parameter constraints in Equation (35). The sliding mode control law $\mathbf{u}$ is updated by the model predictive controller at a control interval of $\Delta t = 1$ s and the prediction horizon is $N = 30$.

Figure 9 presents the resulting USV paths for all three cases and the tracking error d is presented in Figure 10. The control parameter evolution is presented graphically in Figure 11. The initial optimization yields a 26% performance gain over the base case but the MPC cascade structure only yields another 4% cost improvement over the initial optimization. Since the inequality constraint on control is not active in this case, the optimal controller parameters can be implemented from time $t = 0$ and do not change significantly as the simulation progresses. It is interesting to note, however, that the MPC cascade structure decreases the reach time as well as the integral squared effort cost.

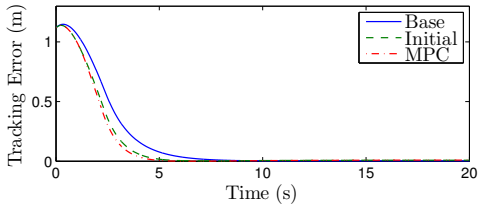

Fig. 7. Minimum time tracking error: Circular trajectory

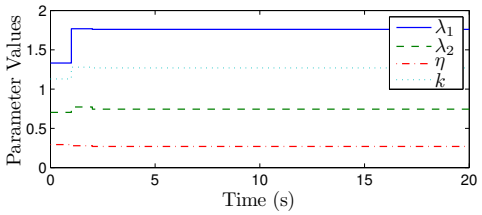

Fig. 8. Minimum time parameter evolution: Circular trajectory

V. Conclusions

An optimizing sliding mode cascade control structure was presented to determine the surface parameters for sliding mode control of underactuated Unmanned Surface Vessels. A discrete-time, nonlinear model predictive controller was used to update the parameters of the sliding mode control surfaces in order to achieve minimum tracking error, minimum time, and minimum energy objectives. The vessel trajectories were shown to be significantly improved in each optimization case for a desired typical circular motion. Future work will include additional trajectories and experimental implementation.

Acknowledgment

This research was originated and supervised by our late colleague Professor Kenneth R. Muske. Support for this work from the Office of Naval Research under ONR Grant N00014-04-1-0642 and the Center for Nonlinear Dynamics and Control (CENDAC) at Villanova University is gratefully acknowledged.

References

[1] V.I. Utkin. Variable structure systems with sliding modes. *IEEE Transactions on Automatic Control*, 22(2):212–222, 1977.

[2] M. Salamci, M. Ozgoren, and S. Banks. Sliding mode control with optimal sliding surfaces for missile autopilot design. *Journal of Guidance, Control, and Dynamics*, 23:719–727, 2000.

[3] B. Eksin, S. Tokat, M. Guzelkaya, and M. Soylemez. Design of a sliding mode controller with a nonlinear time-varying sliding surface. *Transactions of the Institute of Measurement and Control*, 25:145–162, 2003.

[4] K. S. Kim and Y. Park. Sliding mode design via quadratic performance optimization with pole-clustering constraint. *SIAM Journal on Control and Optimization*, 43:670–684, 2004.

[5] M. Nikkhah, H. Ashrafiuon, and K. Muske. Optimal sliding control for underactuated systems. In *Proceedings of the 2006 American Control Conference*, pages 4688–4693, 2006.

[6] K. Muske, M. Nikkhah, and H. Ashrafiuon. A predictive and sliding mode cascade controller. In *Proceedings of the 2007 American Control Conference*, pages 4540–4545, 2007.

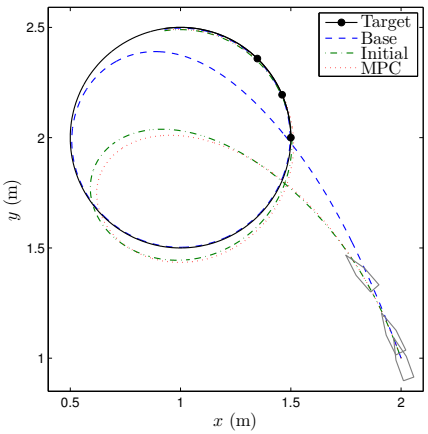

Fig. 9. Simulated minimum energy paths: Circular trajectory

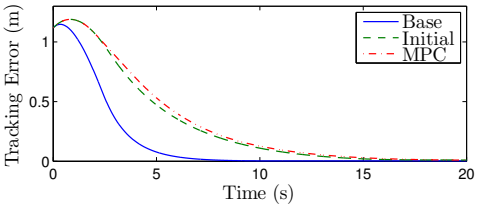

Fig. 10. Minimum energy tracking error: Circular trajectory

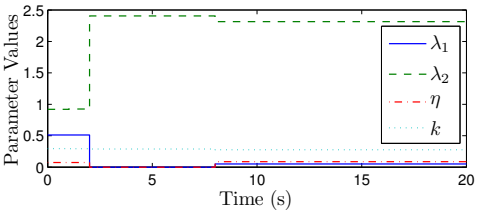

Fig. 11. Minimum energy parameter evolution: Circular trajectory

[7] L. McNinch, H. Ashrafiuon, and K. Muske. Optimal specification of sliding mode control parameters for unmanned surface vessel systems. In *Proceedings of the 2009 American Control Conference*, pages 2350–2355, 2009.

[8] H. Ashrafiuon and R. Erwin. Sliding mode control of underactuated multibody systems and its application to shape change control. *International Journal of Control*, 81(12):1849–1858, 2008.

[9] D. Mayne, J. Rawlings, C. Rao, and P. Skocart. Constrained model predictive control: Stability and optimality. *Automatica*, 36(6):789–814, 2000.

[10] H. Ashrafiuon, K.R. Muske, L.C. McNinch, and R.A. Soltan. Sliding-mode tracking control of surface vessels. *IEEE Transactions on Industrial Electronics*, 55(11):4004–4012, 2008.

[11] T.I. Fossen. *Guidance and Control of Ocean Vehicles*. Wiley, New York, 1994.

[12] K.R. Muske, H. Ashrafiuon, G. Haas, G. McCloseky, and T. Flynn. Identification of a control oriented nonlinear dynamic usv model. In *Proceedings of the 2008 American Control Conference*, pages 562–567, 2008.

[13] H. Khalil. *Nonlinear Systems*. Prentice-Hall, Upper Saddle River, NJ, 1996.

[14] A. Bryson and Y. Ho. *Applied Optimal Control*. Taylor & Francis, Levittown, PA, revised edition, 1975.